Ni, YQ, Fan, KQ, Zheng, G, Chan, Tommy, & Ko, JM
(2003)
Automatic modal identification of cable-supported bridges instrumented with a long-term monitoring system.
In Kiu, S C (Ed.) *Proceedings of Smart Structures and Materials 2003: Smart Systems and Nondestructive Evaluation for Civil Infrastructures.*
International Society for Optical Engineering (SPIE), United States of America, pp. 329-339.

https://doi.org/10.1117/12.482379

Ni, Y.Q. and Fan, K.Q. and Zheng, G. and Chan, Tommy H.T. and Ko, J.M. (2003) Automatic modal identification of cable-supported bridges instrumented with a long-term monitoring system. In Liu, S.C., Eds. Proceedings Smart Structures and Materials 2003: Smart Systems and Nondestructive Evaluation for Civil Infrastructures 5057, pages pp. 329-339.

Automatic modal identification of cable-supported bridges instrumented with a long-term monitoring system

Y. Q. Ni[*a], K. Q. Fan[b], G. Zheng[c], T. H. T. Chan[a], J. M. Ko[a]
[a]Dept. of Civil and Structural Engineering, The Hong Kong Polytechnic University, Hong Kong;
[b]School of Information, Wuyi University, Jiangmen, Guangdong, P. R. China 529020;
[c]Chongqing Communications Research and Design Institute, Chongqing, P. R. China 400067

ABSTRACT

An automatic modal identification program is developed for continuous extraction of modal parameters of three cable-supported bridges in Hong Kong which are instrumented with a long-term monitoring system. The program employs the Complex Modal Indication Function (CMIF) algorithm to identify modal properties from continuous ambient vibration measurements in an on-line manner. By using the LabVIEW graphical programming language, the software realizes the algorithm in Virtual Instrument (VI) style. The applicability and implementation issues of the developed software are demonstrated by using one-year measurement data acquired from 67 channels of accelerometers deployed on the cable-stayed Ting Kau Bridge. With the continuously identified results, normal variability of modal vectors caused by varying environmental and operational conditions is observed. Such observation is very helpful for selection of appropriate measured modal vectors for structural health monitoring applications.

Keywords: automatic modal identification, complex modal indication function, modal vector, environmental variability

1. INTRODUCTION

Real-time or near real-time damage monitoring of civil infrastructure systems when subjected to natural or man-made disasters has widespread societal implications. Not only does this give infrastructure owners/mangers knowledge of what and where damage may have occurred, but also whether immediate evacuation of the occupants/contents is necessary. For three key bridges in Hong Kong, a sophisticated on-structure instrumentation system consisting of over 800 sensors has been permanently installed for continuous on-line structural monitoring [1, 2]. The large volume of collected data from a continuous monitoring system involving hundreds of sensors makes manual probing almost impossible. Especially, traditional human analysis leads to the breakdown of real-time or near real-time monitoring. Automatic and on-line data processing and analysis is therefore imperative for real-time or near real-time structural health monitoring.

This paper describes the development of an automatic modal identification program and its application to the cable-stayed Ting Kau Bridge. Software that can automatically identify modal properties from continuous ambient vibration measurement is developed in the LabVIEW environment. The Complex Modal Indication Function (CMIF) algorithm is encoded into the software for modal parameter extraction, which is realized in Virtual Instrument (VI) style with the aid of a visualization program. The developed software is then applied for continuous modal parameter identification, at one-hour intervals, of the cable-stayed Ting Kau Bridge by using one-year measurement data from 45 accelerometers (a total of 67 channels) permanently installed on the bridge. From the point of view of structural health monitoring, it is extremely important to discriminate abnormal changes in modal features caused by structural damage from normal changes due to varying environmental and operational conditions [3-12], so that the normal changes will not raise a false positive alarm in health monitoring. It has been accepted that monitoring of structures for at least one complete cycle of in-service/operating environment to include the whole range of environmental conditions is in need before reliably implementing damage identification methods. With a series of modal parameters identified by using the developed software, the environmental variability of modal vectors of the Ting Kau Bridge is observed. From this observation, stationary and non-stationary modes with respect to environmental effects are classified and only the former will be used in damage detection applications. This observation also provides information on appropriate sensor installation locations. Only the results regarding modal vectors are shown in this paper, and the observation on environmental variability of modal frequencies is presented in the companion paper [13].

---

[*] ceyqni@polyu.edu.hk; phone 852 2766-6004; fax 852 2334 6389; http://www.cse.polyu.edu.hk/~dynamics/

2. CMIF ALGORITHM AND ITS IMPLEMENTATION

The CMIF algorithm, which was originally proposed for identifying the order of system equation in the frequency domain and the modal parameters from frequency response functions (FRFs) [14, 15], is adapted here to identify modal parameters of large scale bridges with output-only measurements and spatially distributed accelerometers. For a bridge structure with acceleration signals as observation variables, its state-space model can be represented as

$$\begin{aligned} \dot{\boldsymbol{x}}(t) &= \boldsymbol{A}_c \boldsymbol{x}(t) + \boldsymbol{B}_c \boldsymbol{u}(t) \\ \boldsymbol{y}(t) &= \boldsymbol{C}_c \boldsymbol{x}(t) + \boldsymbol{D}_c \boldsymbol{u}(t) \end{aligned} \tag{1}$$

where $\boldsymbol{x} \in \mathbf{R}^{n\times 1}$ is an n-dimensional state vector; $\boldsymbol{y} \in \mathbf{R}^{m\times 1}$ is an m-dimensional output or measurement; $\boldsymbol{u} \in \mathbf{R}^{r\times 1}$ is a r-dimensional control input or excitation. $\boldsymbol{A_c} \in \mathbf{R}^{n\times n}$, $\boldsymbol{B_c} \in \mathbf{R}^{n\times r}$, $\boldsymbol{C_c} \in \mathbf{R}^{m\times n}$ and $\boldsymbol{D_c} \in \mathbf{R}^{m\times r}$ are the transition matrix, input coefficient matrix, output coefficient matrix and transfer matrix of the system, respectively.

If the singular value decomposition of the transition matrix is $\boldsymbol{A}_c = \boldsymbol{\Psi}\boldsymbol{\Lambda}_c\boldsymbol{\Psi}^{-1}$, Eq. (1) can be written as

$$\begin{aligned} \dot{\boldsymbol{x}}_m(t) &= \boldsymbol{\Lambda}_c \boldsymbol{x}_m(t) + \boldsymbol{L}_c^T \boldsymbol{u}(t) \\ \boldsymbol{y}(t) &= \boldsymbol{V}_c \boldsymbol{x}_m(t) + \boldsymbol{D}_c \boldsymbol{u}(t) \end{aligned} \tag{2}$$

where $\boldsymbol{L}_c^T = \boldsymbol{\Psi}^{-1}\boldsymbol{B}_c$, $\boldsymbol{V}_c = \boldsymbol{C}_c\boldsymbol{\Psi}$, and the diagonal elements of $\boldsymbol{\Lambda}_c$ (i.e. the singular values of $\boldsymbol{A}_c$) are

$$\lambda_k = -\xi_k\omega_k + j\omega_k\sqrt{1-\xi_k^2} \tag{3}$$

in which ω_k and ξ_k are the modal frequency and damping ratio of the kth mode.

If the excitation is assumed to be a zero-mean white noise vector satisfying

$$E[\boldsymbol{u}(t)] = 0\,,\quad \boldsymbol{R}_u(\tau) = E[\boldsymbol{u}(t+\tau)\boldsymbol{u}^T(t)] = \boldsymbol{R}_u\delta(\tau) \tag{4}$$

then the power spectral density matrix of the input can be expressed as

$$\boldsymbol{S}_u(s) = \int_{-\infty}^{\infty}\boldsymbol{R}_u(t)e^{-st}dt = \boldsymbol{R}_u \tag{5}$$

and the power spectral density matrix of the output is obtained as

$$\boldsymbol{S}_y(s) = \boldsymbol{H}_c(s)\boldsymbol{R}_u\boldsymbol{H}_c^T(s^*) \tag{6}$$

where $\boldsymbol{H}_c(s)$ is the transfer function of the system, which is obtained by the Laplace transform of Eq. (1) as

$$\boldsymbol{H}_c(s) = \frac{\boldsymbol{Y}(s)}{\boldsymbol{u}(s)} = \boldsymbol{C}_c(s\boldsymbol{I} - \boldsymbol{A}_c)^{-1}\boldsymbol{B}_c + \boldsymbol{D}_c \tag{7}$$

where $\boldsymbol{Y}(s)$ and $\boldsymbol{u}(s)$ are the Laplace transforms of the output and input, respectively. By expressing the transfer function in pole-residue form, we have

$$\boldsymbol{H}_c(s) = \sum_{k=1}^{n}\frac{s^2}{\lambda_k^2(s-\lambda_k)}\{\boldsymbol{v}_{ck}\}\{\boldsymbol{l}_{ck}\}^T \tag{8}$$

where $\{\boldsymbol{v}_{ck}\} \in \mathbf{R}^{m\times 1}$ is the kth modal vector; $\{\boldsymbol{l}_{ck}\} \in \mathbf{R}^{r\times 1}$ is the kth modal participation factor vector; λ_k is the system pole value of the kth mode. Upon the substitution of Eq. (8) in Eq. (6), we obtain

$$\boldsymbol{S}_y(s) = \left\{\sum_{k=1}^{n}\frac{s^2}{\lambda_k^2(s-\lambda_k)}\{\boldsymbol{v}_{ck}\}\{\boldsymbol{l}_{ck}\}^T\right\}\boldsymbol{R}_u\left\{\sum_{k=1}^{n}\frac{(s^*)^2}{\lambda_k^2(s^*-\lambda_k)}\{\boldsymbol{l}_{ck}\}\{\boldsymbol{v}_{ck}\}^T\right\} \tag{9}$$

It is seen from Eq. (9) that $\boldsymbol{S}_y(s)$ reaches its extreme when $s = -\xi_k\omega_k + j\omega_k\sqrt{1-\xi_k^2}$. In the case of weak damping, the value of $\boldsymbol{S}_y(s)|_{s=j\omega_k}$ mainly depends on the kth mode. By neglecting the effects from other modes, we have

$$\boldsymbol{S}_y(j\omega_k) \approx \frac{\{\boldsymbol{v}_{ck}\}\{\boldsymbol{l}_{ck}\}^T\boldsymbol{R}_u\{\boldsymbol{l}_{ck}^*\}\{\boldsymbol{v}_{ck}^*\}^T}{(\xi_k\omega_k)^2} = \{\boldsymbol{v}_{ck}\}\alpha_k\{\boldsymbol{v}_{ck}^*\}^T \tag{10}$$

where the complex scalar quantity α_k is given by

$$\alpha_k = \frac{\{\boldsymbol{l}_{ck}\}^T \boldsymbol{R}_u \{\boldsymbol{l}_{ck}^*\}}{(\xi_k \omega_k)^2} \tag{11}$$

Taking the singular value decomposition of $\boldsymbol{S}_y(s)$ at $s = j\omega_k$ yields

$$\boldsymbol{S}_y(j\omega_k) = \boldsymbol{U}(j\omega_k)\Sigma(j\omega_k)[\boldsymbol{U}^*(j\omega_k)]^T \tag{12}$$

where $\boldsymbol{U}(j\omega_k) = [\boldsymbol{u}_1 \;\; \boldsymbol{u}_2 \;\; \cdots \;\; \boldsymbol{u}_m]$ and $\boldsymbol{u}_k$ is the column vector of $\boldsymbol{U}(j\omega_k)$; $\Sigma(j\omega_k) = diag[s_1 \; s_2 \; \cdots \; s_m]$ and s_i is the singular value ordered in descending sort. The matrix $\Sigma(j\omega_k)$ is herein referred to as the complex mode indication function (CMIF).

It is known from Eqs. (10) and (12) that if the value of $\boldsymbol{S}(j\omega)|_{\omega=\omega_k}$ is dominated by one mode, then only the first singular value s_1 out of $\{s_1 \; s_2 \cdots s_m\}$ will reach its maximum. More generally, if the value of $\boldsymbol{S}(j\omega)|_{\omega=\omega_k}$ is dominated by i modes, there will be i singular values which reach their local maxima when ω approaches to ω_k. By setting the remaining (m-i) singular values as zero, the rank of the diagonal matrix $\Sigma(j\omega_k)$ will be equal to number of dominant modes at $\omega = \omega_k$, and consequently, the column vector $\boldsymbol{u}_i$ corresponding to the nonzero singular value s_i in $\boldsymbol{U}(j\omega_k)$ will represent the modal shape of the ith mode. The modal frequencies and modal shapes are thus identified. Because the singular value decomposition process has resulted in the spectral density function for each decomposed single-degree-of-freedom system, the corresponding modal damping can be readily estimated.

The above algorithm has been encoded as a program by using the LabVIEW graphical programming language. With the aid of a visualization program, the automatic modal parameter identification is performed in Virtual Instrument (VI) style. Typical user interfaces of the developed software are shown below. Figure 1 illustrates the time history of response records and the response spectrum diagrams. Figure 2 shows the extracted complex mode indication functions and the identified modal shape.

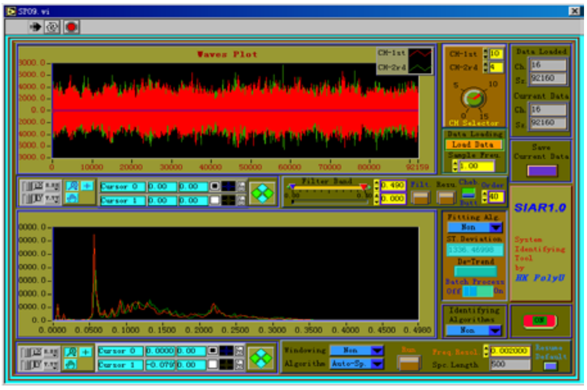

Figure 1: Time-domain response and power spectral density

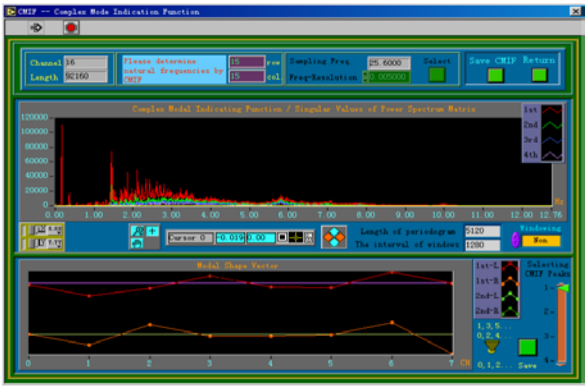

Figure 2: Illustration of CMIF and modal shape

3. APPLICATION TO TING KAU BRIDGE

The Ting Kau Bridge, as shown in Figure 3, is a three-tower cable-stayed bridge with two main spans of 448 m and 475 m respectively, and two side spans of 127 m each [16]. A sophisticated long-term monitoring system consisting of over 230 sensors has been installed on the bridge immediately after completion of its construction [1, 2]. The sensors include accelerometers, strain gauges, displacement transducers, anemometers, temperature sensors, weigh-in-motion sensors, and recently deployed global positioning system (GPS) [17]. 24 uni-axial accelerometers, 20 bi-axial accelerometers and 1 tri-axial accelerometer (totally 67 accelerometer channels) are permanently deployed at the deck of the two main spans and the two side spans, the longitudinal stabilizing cables, the top of the three towers, and the base of central tower to monitor seismic excitation and dynamic response of the bridge. One-year continuously acquired acceleration data from all these 67 channels, covering one full cycle of in-service/operating conditions, are used herein for modal parameter identification and environmental variability observation.

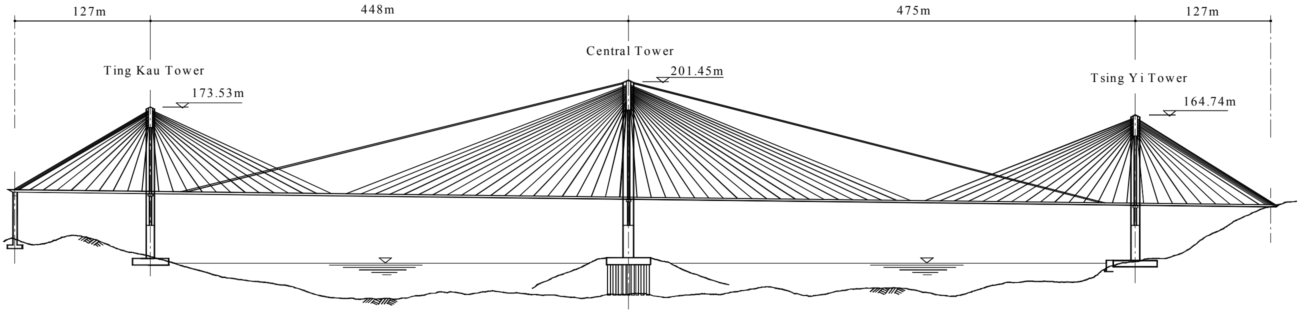

Figure 3: Elevation of Ting Kau Bridge

Table 1 gives the accelerometer installation information. Notation of the senor locations (numbering of bridge cross-sections) refers to the references [1, 2]. The category 'Cable-TK' implies the sensors installed on the longitudinal stabilizing cables in the Ting Kau main span, and 'Cable-TY' indicates the sensors installed on the longitudinal stabilizing cables in the Tsing Yi main span. The indices 'X', 'Y' and 'Z' denote the longitudinal, lateral and vertical directions, respectively. The accelerometers on the cables were positioned in vertical and lateral directions. The accelerometers on the deck were also installed in vertical direction (at both deck edges) and lateral direction (at central girder). For the bridge towers, the accelerometers were mainly deployed in longitudinal (along the bridge axis) and lateral (sway) directions except for one accelerometer channel being oriented in vertical direction for seismic excitation measurement at the base of central tower. All signals from the 67 accelerometer channels were acquired with a sampling rate of 25.6 Hz through 24-hour continuous monitoring per day. One-year data have been used for this investigation and modal analysis was conducted using the developed software at one-hour intervals. Figures 4 and 5 show the identified CMIFs and mode shapes for a typical vertical mode and a typical torsional mode of the bridge. Only the vertical modal vectors of measurement points at two edges of the deck are plotted in the figures. They are obtained by using one-hour response records during 4:00 to 5:00 pm of 1 March 1999.

Table 1. Information of accelerometers installed

Cable_TK		Cable_TY		Deck_vertical		Deck_lateral		Tower	
Ch ID	Location	Ch ID	Location	Ch ID	Location	Ch ID	Location	Ch ID	Location
BGFC1Z	11718	BGKC1Z	12187	SGBE1Z	11429	SGBW2Y	11429	BGCT1X	11505
BGFC1Y	11718	BGKC1Y	12187	SGBW1Z	11429	SGDW2Y	11580	BGCT1Y	11505
BGFC2Z	11718	BGKC2Z	12187	SGDE1Z	11580	SGEW2Y	11688	BGHT1X	11953
BGFC2Y	11718	BGKC2Y	12187	SGDW1Z	11580	SGGW2Y	11823	BGHT1Y	11953
BGFC3Z	11718	BGKC3Z	12187	SGEE1Z	11688	SGJW2Y	12082	BGHT2X	11953
BGFC3Y	11718	BGKC3Y	12187	SGEW1Z	11688	SGLW2Y	12217	BGHT2Y	11953
BGFC4Z	11718	BGKC4Z	12187	SGGE1Z	11823	SGMW2Y	12352	TGHT1X	11953
BGFC4Y	11718	BGKC4Y	12187	SGGW1Z	11823	SGOW2Y	12503	TGHT1Y	11953
BGFC5Z	11718	BGKC5Z	12187	SGJE1Z	12082			TGHT1Z	11953
BGFC5Y	11718	BGKC5Y	12187	SGJW1Z	12082			BGNT1X	12428
BGFC6Z	11718	BGKC6Z	12187	SGLE1Z	12217			BGNT1Y	12428
BGFC6Y	11718	BGKC6Y	12187	SGLW1Z	12217				
BGFC7Z	11718	BGKC7Z	12187	SGME1Z	12352				
BGFC7Y	11718	BGKC7Y	12187	SGMW1Z	12352				
BGFC8Z	11718	BGKC8Z	12187	SGOE1Z	12503				
BGFC8Y	11718	BGKC8Y	12187	SGOW1Z	12503				

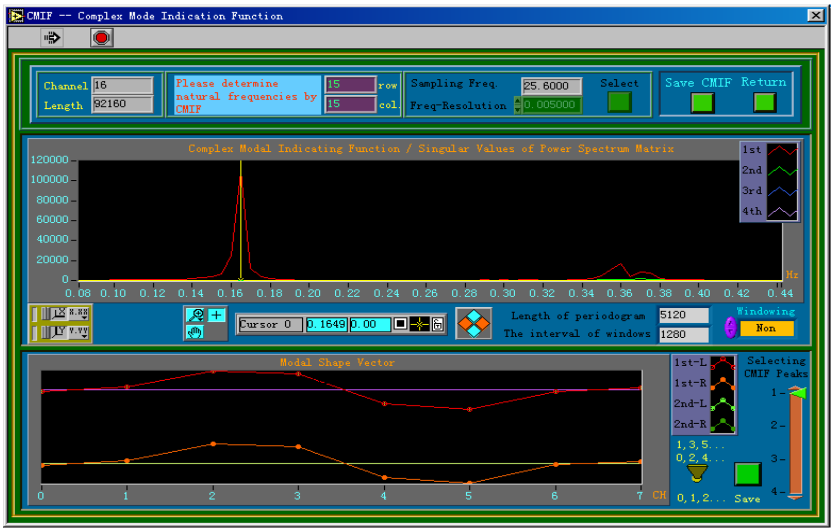
CMIF -- Complex Mode Indication Function

Channel 16
Length 92160
Please determine natural frequencies by CMIF
15 row
15 col
Sampling Freq. 25.6000
Freq-Resolution 0.005000
Cursor 0 0.1649 0.00
Length of periodogram 5120
The interval of windows 1280
Windowing Non

Figure 4: Identified CMIF and modal shape for a typical vertical mode

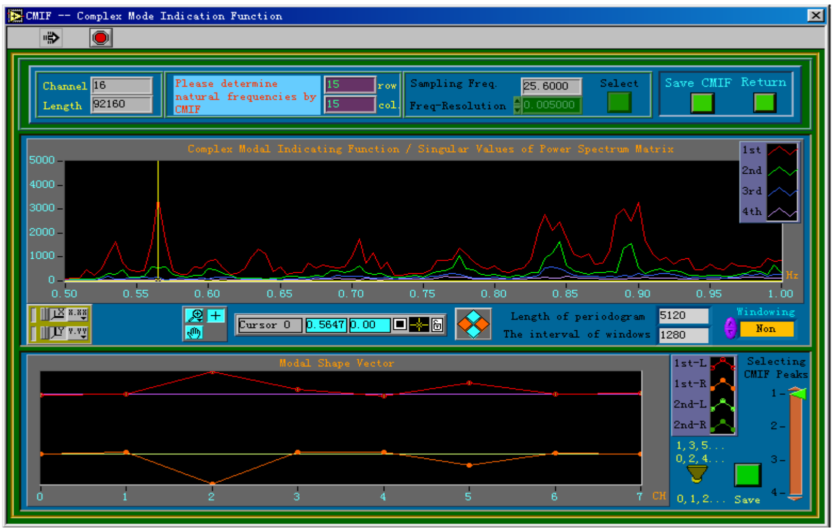
CMIF -- Complex Mode Indication Function

Channel 16
Length 92160
Please determine natural frequencies by CMIF
15 row
15 col
Sampling Freq. 25.6000
Freq-Resolution 0.005000
Cursor 0 0.5647 0.00
Length of periodogram 5120
The interval of windows 1280
Windowing Non

Figure 5: Identified CMIF and modal shape for a typical torsional mode

Figures 6 to 10 show the modal identification results for some low-frequency global modes. In each of the figures, the left upper graph shows the deck vertical modal components at western and eastern edges and the deck lateral modal components; the left lower graph plots the natural frequencies identified at different times for an identical mode; and the right graph illustrates the lateral (sway) motions of the cables, towers and deck. It is found that the first mode of the Ting Kau Bridge is a predominantly vertical mode with its natural frequency $f = 0.165$ Hz, which is less than the first modal frequency (0.199 Hz) of the world's longest cable-stayed Tatara Bridge [18]. It implies that the Ting Kau Bridge is one of the most flexible cable-stayed bridges in the world. The bridge has the first predominantly torsional mode at the natural frequency $f = 0.228$ Hz and the first predominantly lateral mode at the natural frequency $f = 0.262$ Hz. Due to the extremely long longitudinal stabilizing cables (up to 465 m), slender monoleg towers and separated deck system, the bridge exhibits strong modal coupling and interaction. For example, the first predominantly torsional mode is coupled with lateral modal components as shown in Figure 7, and the first predominantly lateral mode incorporates torsional modal components as shown in Figure 8. Significant modal interaction between the deck, towers and cables is observed. In the first predominantly vertical mode, for instance, besides both the deck and central tower participating greatly in the modal motion, the longitudinal stabilizing cables vibrate with very large amplitude.

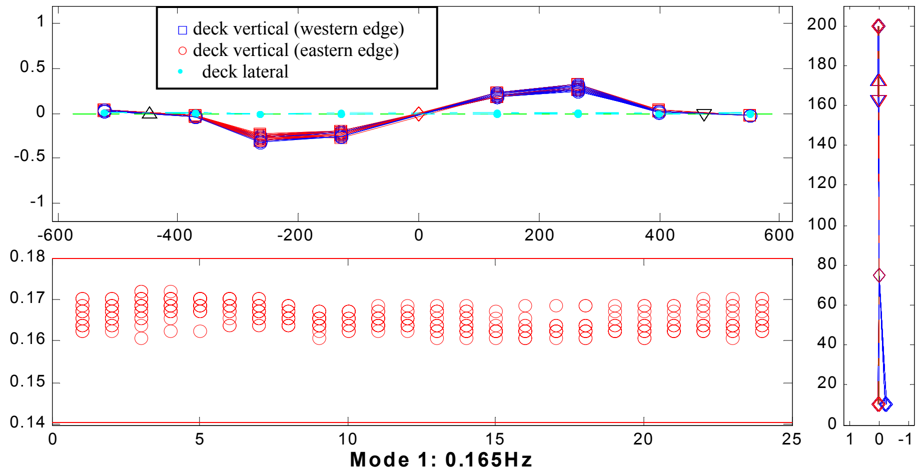

Figure 6: Measured modal vectors and natural frequencies of the 1st mode

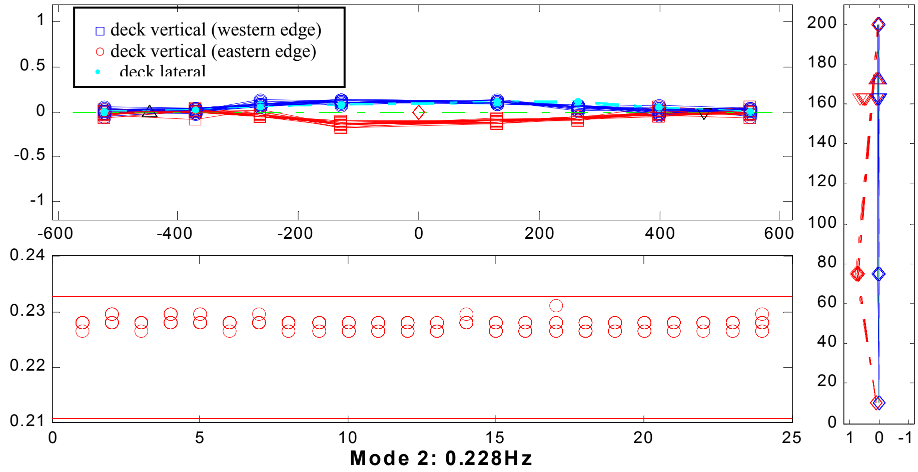

Figure 7: Measured modal vectors and natural frequencies of the 2nd mode

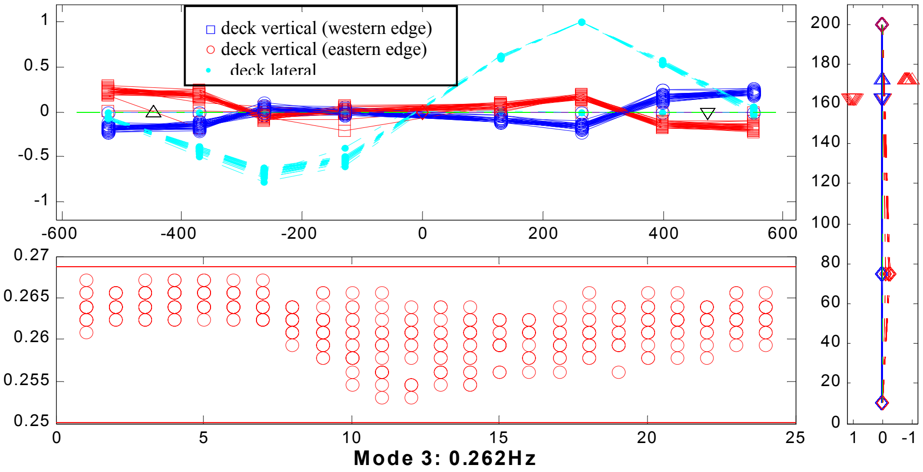

Figure 8: Measured modal vectors and natural frequencies of the 3rd mode

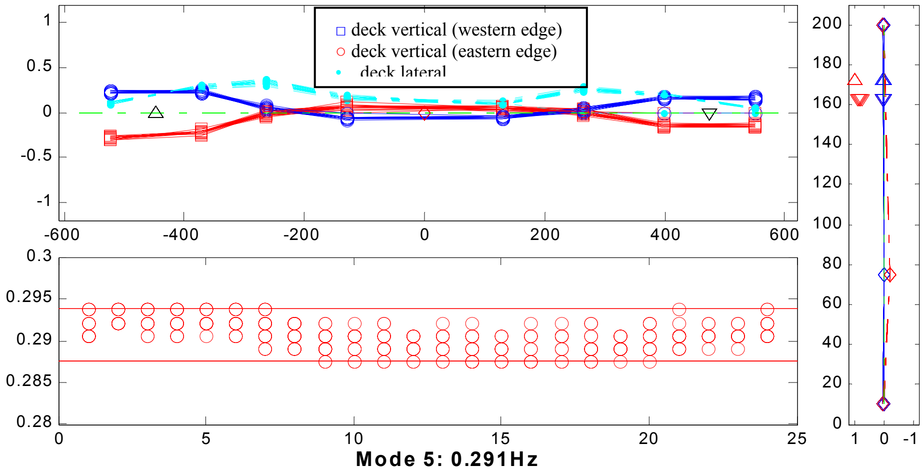

Figure 9: Measured modal vectors and natural frequencies of the 5th mode

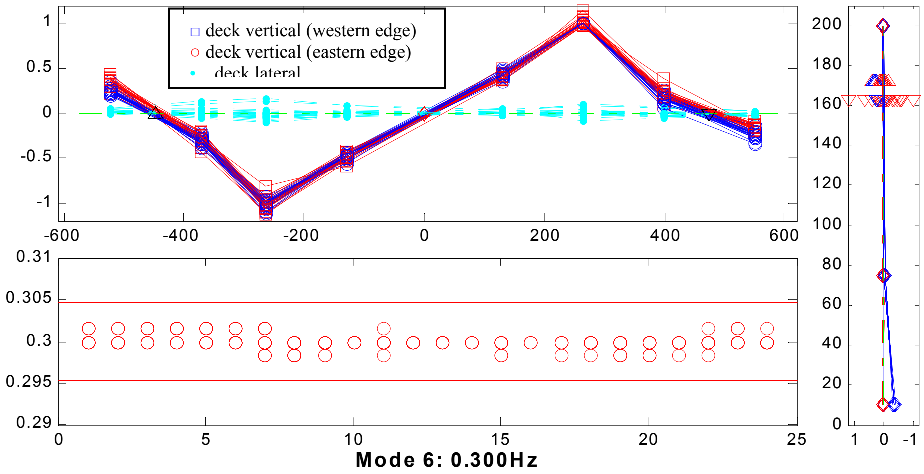

Figure 10: Measured modal vectors and natural frequencies of the 6th mode

4. ENVIRONMENTAL VARIABILITY OF MODAL VECTORS

Following the vibration-based structural health monitoring approach, damage in a structure is identified from changes in selected modal features extracted from the vibration measurements. However, most civil structures are directly exposed to the environment and are thus subjected to variations in temperature, humidity, wind, traffic, insolation as well as other influences. These varying environmental and operational conditions also cause changes in modal features which may mask subtler structural changes caused by damage. Environmental variability in modal parameters must be considered before reliable use of modal-based damage detection methods. A thorough understanding of this variability is necessary so that changes in modal features resulting from damage can be discriminated from changes resulting from such variability. Considerable research efforts have been devoted to investigating the variability of modal frequencies caused by in-service environmental and operational conditions [3-12], but no study addressing the environmental variability of modal vectors was reported. Because the modal vector information is necessary for locating structural damage, the environmental variability of modal vectors is observed in the present study.

Figures 11 to 15 show 100 samples of measured modal vectors corresponding to the modes shown in Figures 6 to 10. For clarity only the modal vectors of the measurement points at the deck are plotted. The 100 samples cover the measurements in February, March, July, August, October and December 1999. For each sample, one-hour acceleration data are used to identify a set of modal frequencies and modal vectors by means of the developed software.

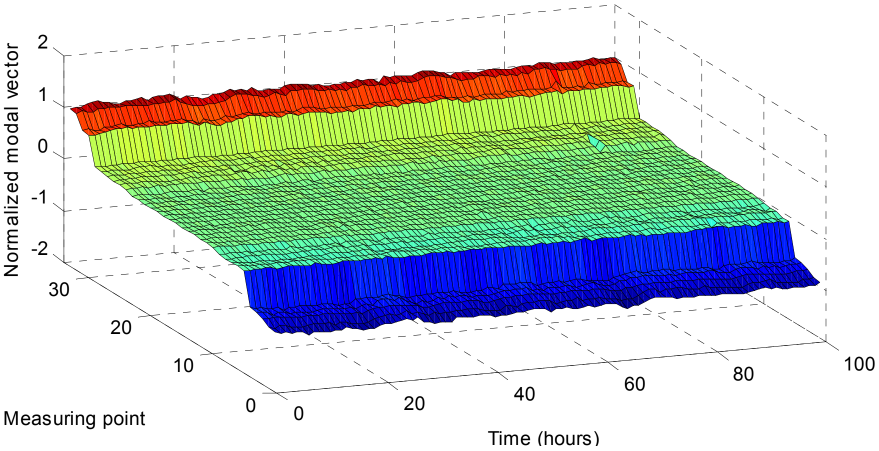

Figure 11: Environmental variability of modal vectors for the 1st mode

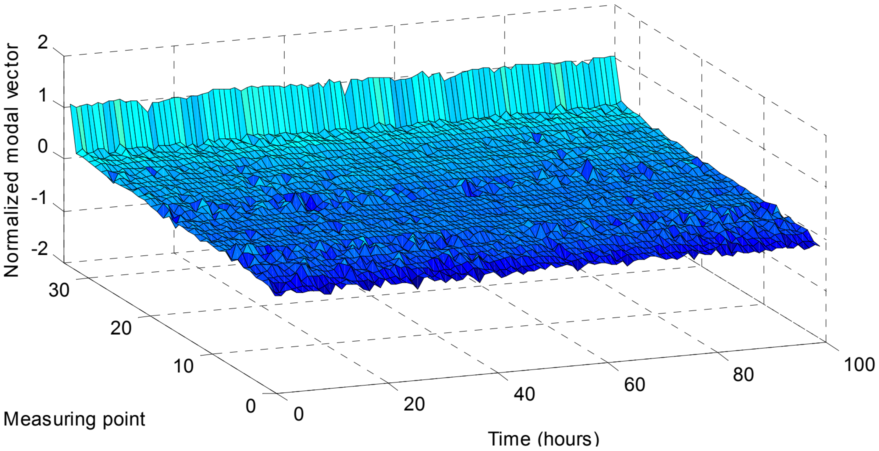

Figure 12: Environmental variability of modal vectors for the 2nd mode

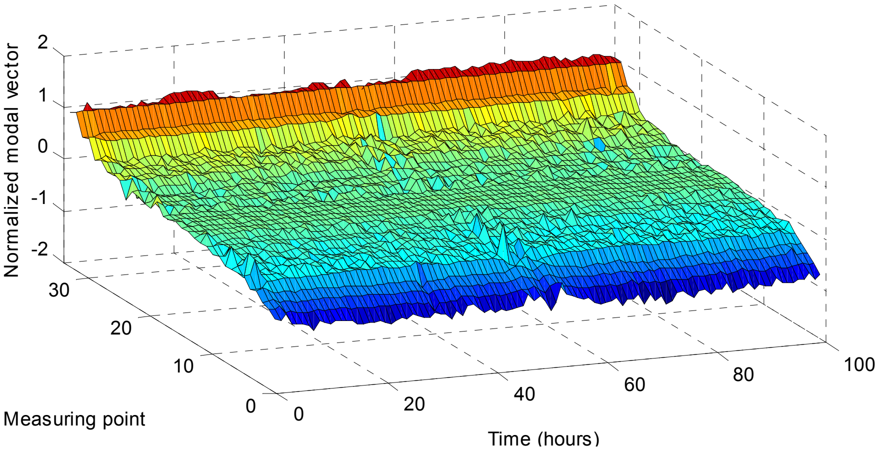

Figure 13: Environmental variability of modal vectors for the 3rd mode

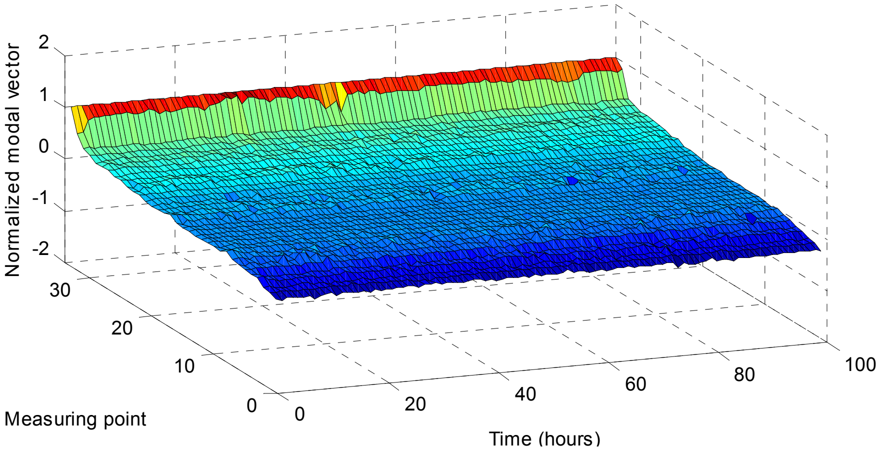

Figure 14: Environmental variability of modal vectors for the 5th mode

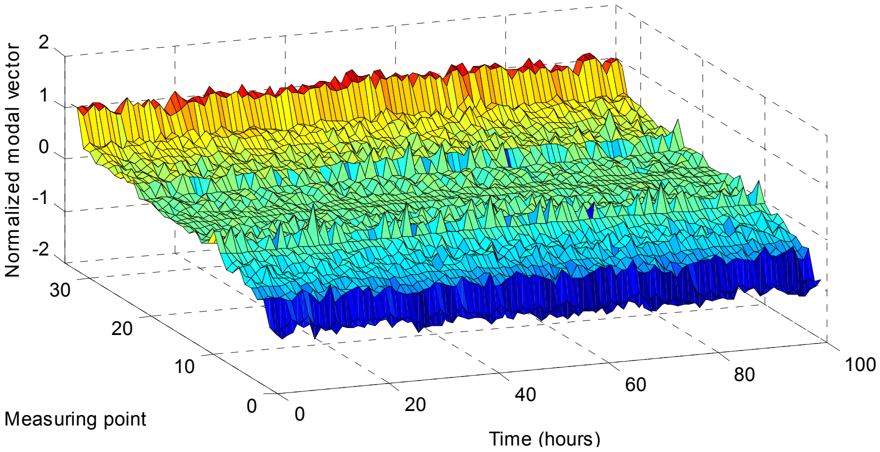

Figure 15: Environmental variability of modal vectors for the 6th mode

It is observed from Figures 11 to 15 that the environmental variability has different levels for different modes. The modal vectors for the 1st and 5th modes exhibit very good stationarity for all the measurement points under varying environmental and operational conditions. It is therefore concluded that using modal information of these two modes will provide most reliable damage identification results. For the 2nd and 3rd modes, the modal vectors at some locations are found to be fairly stationary but the others exhibit noticeable non-stationarity. The environmental variability level of modal vectors for the 6th mode is considerably large. Because changes in modal parameters caused by structural damage are usually insignificant, such environmental variability level may be greater than the modal parameter variation caused by structural damage. Therefore, these measured modal parameters can be used for damage detection without false identification only after the non-stationarity of the modal parameters is quantified and the changes caused by environmental variations are discriminated from those caused by structural damage. In summary, an observation of environmental variability of modal vectors can select the most appropriate modes used in vibration-based damage identification and determine the sensor positions which are tolerant of environmental variability.

5. CONCLUSIONS

An automatic modal identification program employing the Complex Modal Indication Function (CMIF) algorithm has been developed for modal parameter extraction of the Ting Kau Bridge from continuously acquired ambient vibration response signals. The program accomplishes the data analysis in Virtual Instrument style. With one-year measurement data from 45 accelerometers (a total of 67 channels) which are permanently installed on the bridge as part of a long-term monitoring system, modal parameters of the Ting Kau Bridge under a full cycle of in-service/operating conditions are identified and the variability of modal vectors due to environmental variations is observed. The modal analysis results show that the Ting Kau Bridge exhibits strong modal coupling with simultaneous modal components in the three dimensions and significant modal interaction among the deck, towers and cables. Observation on the environmental variability of modal vectors indicates that the variability level is different for different modes. Using modal information of the modes with small environmental variability can provide reliable structural damage identification. For the modes with large environmental variability, the non-stationarity of the modal parameters must be quantified before modal-based damage detection methods can be reliably applied to monitor real structures. A one-year full-cycle observation of the environmental variations can provide useful information on selecting appropriate modes for damage identification and determining sensor positions with high tolerance of environmental variability. Based on the statistical analysis of observed environmental variations, it is possible to discriminate the changes of modal parameters due to environmental factors from those caused by structural damage.

ACKNOWLEDGEMENTS

The work described in this paper was supported in part by a grant from the Research Grants Council of the Hong Kong Special Administrative Region, China (Project No. PolyU 5052/99E) and partially by a grant from the Hong Kong Polytechnic University under the Cross-Departmental Project Fund. The writers also wish to thank the Highways Department of the Hong Kong SAR Government, especially Ir. W.M. Chan, Ir. Dr. K.Y. Wong and Ir. W.Y.K. Chan, for providing support for this research.

REFERENCES

1. C.K. Lau, W.P.N. Mak, K.Y. Wong, W.Y.K. Chan, K.L.D. Man, "Structural health monitoring of three cable-supported bridges in Hong Kong," *Structural Health Monitoring 2000*, F.-K. Chang (ed.), Technomic Publishing Co., Lancaster, Pennsylvania, pp. 450-460, 1999.
2. K.Y. Wong, C.K. Lau, A.R. Flint, "Planning and implementation of the structural health monitoring system for cable-supported bridges in Hong Kong," *Nondestructive Evaluation of Highways, Utilities, and Pipelines IV*, A.E. Aktan and S.R. Gosselin (eds.), SPIE Vol. **3995**, pp. 266-275, 2000.
3. G.P. Roberts, A.J. Pearson, "Dynamic monitoring as a tool for long span bridges," *Bridge Management 3: Inspection, Maintenance, Assessment and Repair*, J.E. Harding, G.E.R. Parke and M.J. Ryall (eds.), E & FN Spon, London, pp. 704-711, 1996.
4. M. Abdel Wahab, G. De Roeck, "Effect of temperature on dynamic system parameters of a highway bridge," *Structural Engineering International*, **7**, pp. 266-270, 1997.
5. C.R. Farrar, S.W. Doebling, P.J. Cornwell, E.G. Straser, "Variability of modal parameters measured on the Alamosa Canyon Bridge," *Proceedings of the 15th International Modal Analysis Conference*, Orlando, Florida, Vol. **1**, pp. 257-263, 1997.
6. S. Alampalli, "Influence of in-service environment on modal parameters," *Proceedings of the 16th International Modal Analysis Conference*, Santa Barbara, California, Vol. **1**, pp. 111-116, 1998.
7. H. Sohn, M. Dzwonczyk, E.G. Straser, A.S. Kiremidjian, K.H. Law, T. Meng, "An experimental study of temperature effect on modal parameters of the Alamosa Canyon Bridge," *Earthquake Engineering and Structural Dynamics*, **28**, pp. 879-897, 1999.
8. G.M. Lloyd, M.L. Wang, V. Singh, "Observed variations of mode frequencies of a prestressed concrete bridge with temperature," *Proceedings of ASCE 14th Engineering Mechanics Conference*, Austin, Texas, 2002 (in CD format).
9. R.G. Rohrmann, M. Baessler, S. Said, W. Schmid, W.F. Ruecker, "Structural causes of temperature affected modal data of civil structures obtained by long time monitoring," *Proceedings of the 18th International Modal Analysis Conference*, San Antonio, Texas, Vol. **1**, pp. 1-7, 2000.
10. B. Peeters, G. De Roeck, "One-year monitoring of the Z24-Bridge: environmental effect versus damage events," *Earthquake Engineering and Structural Dynamics*, **30**, pp. 149-171, 2001.
11. J. Kullaa, "Elimination of environmental influences from damage-sensitive features in a structural health monitoring system," *Proceedings of the 1st European Workshop on Structural Health Monitoring*, D.L. Balageas (ed.), DEStech Publications, Lancaster, Pennsylvania, pp. 742-749, 2002.

12. H. Sohn, K. Worden, C.R. Farrar, “Consideration of environmental and operational variability for damage diagnosis,” *Smart Structures and Materials 2002: Smart Systems for Bridges, Structures, and Highways*, S.-C. Liu and D.J. Pines (eds.), SPIE Vol. **4696**, pp. 100-111, 2002.
13. J.M. Ko, K.K. Chak, J.Y. Wang, Y.Q. Ni, T.H.T. Chan, “Formulation of an uncertainty model relating modal parameters and environmental factors by using long-term monitoring data,” *Smart Structures and Materials 2003: Smart Systems and Nondestructive Evaluation for Civil Infrastructures*, S.-C. Liu (ed.), SPIE Vol. **5057**, 2003.
14. C.Y. Shih, Y.G. Tsuei, R.J. Allemang, D.L. Brown, “A frequency domain global parameter estimation method for multiple reference frequency response measurements,” *Mechanical Systems and Signal Processing*, **2**, pp. 349-365, 1988.
15. C.Y. Shih, Y.G. Tsuei, R.J. Allemang, D.L. Brown, “Complex mode indication function and its applications to spatial domain parameter estimation,” *Mechanical Systems and Signal Processing*, **2**, pp. 367-377, 1988.
16. R. Bergermann, M. Schlaich, “Ting Kau Bridge, Hong Kong,” *Structural Engineering International*, **6**, pp. 152-154, 1996.
17. K.Y. Wong, K.L. Man, W.Y. Chan, “Application of global positioning system to structural health monitoring of cable-supported bridges,” *Health Monitoring and Management of Civil Infrastructure Systems*, S.B. Chase and A.E. Aktan (ed.), SPIE Vol. **4337**, pp. 390-401, 2001.
18. T. Endo, T. Iijima, A. Okukawa, M. Ito, “The technical challenge of a long cable-Stayed bridges–Tatara Bridge,” *Cable-Stayed Bridges: Recent Developments and their Future*, M. Ito, Y. Fujino, T. Miyata and N. Narita (eds.), Elsevier Science Publishers, Amsterdam, Netherlands, pp. 417-436, 1991.
19. Y.Q. Ni, J.Y. Wang, J.M. Ko, “Modal interaction in cable-stayed Ting Kau Bridge,” *Advances in Structural Dynamics*, J.M. Ko and Y.L. Xu (eds.), Elsevier Science Ltd, Oxford, UK, Vol. **1**, pp. 537-544, 2000.